Available online at www.sciencedirect.com
SCIENCE DIRECT®
Journal of Chromatography A, 1053 (2004) 151–159
JOURNAL OF CHROMATOGRAPHY A
www.elsevier.com/locate/chroma

Improved liquid chromatography–mass spectrometry performance in quantitative analysis using a nanosplitter interface

Christine L. Andrews[a,1], Chung-Ping Yu[b], Eric Yang[b], Paul Vouros[a,*]

[a] *Department of Chemistry and Chemical Biology and Barnett Institute, Northeastern University, 102 Hurtig Hall, 360 Huntington Avenue, Boston, MA 02115, USA*

[b] *Worldwide Bioanalysis, Drug Metabolism and Pharmacokinetics, GlaxoSmithKline Pharmaceuticals, King of Prussia, PA 19406, USA*

Abstract

Several pairs of analytes in plasma were investigated to demonstrate the successful utility of a novel interface in quantitative bioanalytical LC–MS and LC–MS/MS. Recently in our laboratory, an interface (the nanosplitter) was developed that allows the coupling of normal-bore liquid chromatography with microelectrospray mass spectrometry. The post-column concentric split minimizes turbulence and is shown to produce significant gains in the mass spectrometric signal. This configuration of the splitter allows sampling of the center portion of the parabolic HPLC plug, which maintains chromatographic integrity while producing high split ratios and effectively conserving nearly 99.9% of the sample. When utilizing a Finnigan mass spectrometer (with a heated capillary interface design), the signal gain with the nanosplitter ranged from 5 to 16 times the peak area obtained using the conventional interface without splitting. The linearity of the nanosplitter and conventional interface are shown to be comparable for all analytes tested. The nanosplitter was also fitted to a Sciex mass spectrometer and the results were compared to those from turbo ionspray. While in this case no significant signal improvement was observed, when normalized to the actual analyte mass introduced into the MS, the mass sensitivity was still increased 270-fold. The variations in signal gain utilizing the nanosplitter on instruments from different manufacturers reflect the inherent differences in the source designs while confirming the benefits of coupling high flow LC separations with low flow mass spectrometric detection.

Keywords: Drug discovery; Concentric post-column splitting; Quantitative analysis; Protein-precipitated plasma samples; Ion suppression

1. Introduction

Liquid chromatography–mass spectrometry (LC–MS) is the premier analytical tool in the pharmaceutical industry. LC–MS is used qualitatively to verify the identity of new chemical entities, to identify biotransformation products and to quantify drugs in biological matrices such as urine and plasma. In many cases, the union of LC and MS may not be straightforward since the optimization of one module may lead to the de-optimization of the other. For instance, fast, high efficiency LC separations can be accomplished on short, large bore columns; however, the high flow rate required often decreases the sensitivity of the mass spectrometric detection [1–3]. To avoid this, the interface between the two methodologies must serve as a buffer zone so that each element may be optimized independently [4].

Traditionally, simple post-column splits have been used to provide a high flow rate for the LC separation and a low flow rate for the MS detection [5–10]. The type of splitter can have an important impact on the success of an LC–MS analysis. Splitting is often accomplished through the use of "T" or "Y" configurations, which can generate a large amount of turbulence at the split point, introducing band broadening and other deleterious chromatographic effects. Instead of an angular split, it is also possible to split flow by placing a tube inside a larger bore tube, thus having the split occur at the entrance of the inner tube, along the same axis as the original flow. Recently in our laboratory, an interface was developed that combines a post-column splitter with an electrospray in-

* Corresponding author. Tel.: +1 617 373 2840; fax: +1 617 373 8478.
E-mail address: p.vouros@neu.edu (P. Vouros).
[1] Present address: Molecular Oncology Research Institute, Tufts-New England Medical Center, Boston, MA 02111, USA.

0021-9673/$ – see front matter © 2004 Elsevier B.V. All rights reserved.
doi:10.1016/j.chroma.2004.08.076

terface [11]. The interface, termed a nanosplitter, utilizes a fused silica transfer capillary as the inner tube of the concentric split and the microelectrospray tip of the ionization source. The flow through the capillary is greatly reduced from that exiting the LC column (approximately 2000:1), thus allowing normal-bore liquid chromatography to be coupled to microelectrospray mass spectrometry in a manner that exploits the benefits of each technique. This interface has been previously shown to decrease ion suppression and increase the mass spectrometric signal-to-noise ratio of drug metabolites from rat hepatocyte incubations.

Microelectrospray provides a number of advantages over conventional electrospray mass spectrometry [12,13] that are especially important in pharmaceutical analyses where complex matrices present in biological fluids can interfere with analyte detection due to ion suppression [14]. Many studies have been conducted recently to investigate ion suppression in LC–MS [14–20] and its effects in drug discovery [21] and pharmacokinetics studies [22–25]. It has been shown that the decreased droplet size in microelectrospray, and associated features such as increased surface area/volume ratio and higher charge/volume ratio, can play a significant role in the degree of ion suppression [15,26,27].

While capillary LC (capLC) coupled to microelectrospray mass spectrometry may provide the sensitivity that is required by pharmaceutical researchers, the difficulties associated with the methodology are well known [1,12]. Matrix components, such as non-volatile salts, dosing vehicles and endogenous components can foul the instrumentation and clog the column or the microelectrospray tip. Additional mechanical obstacles such as pressure fluctuations, bubble formation, and flow rate and spray instability may further complicate its routine use. The longer capLC run time is another major drawback for the high throughput bioanalytical assay. These impediments have driven the pharmaceutical industry to pursue other varieties of LC–MS [28,29] and variations on traditional capLC–MS [30]. In quantification studies, pharmaceutical compounds are typically run at high flow rates through short (2–5 cm) normal-bore columns. For the best results, these assays often require rigorous sample clean-up [18,31–33], the use of column switching [2,34,35] and/or the addition of post-column additives [34–38] to assist in desorption and ionization of the analytes.

Several experiments were designed and conducted to investigate the effects of concentric post-column splitting on the analyses of pharmaceutical compounds. The focus of the first experiment was to evaluate direct charge competition in mixtures at differing flow rates and its effect on signal intensity and dynamic range. In the second and third sets of experiments, plasma extracts were used to determine the influence of the matrix on linearity and dynamic range of quantitative analyses which utilized the nanosplitter, when compared to the instrument's standard interface. The data were used to construct calibration curves for the standard interface LC–MS and the nanosplitter LC–MS. The latter studies also investigated the performance of the nanosplitter on a mass spectrometer with a different source design than previously shown.

2. Experimental

2.1. The nanosplitter

Fig. 1 provides a schematic depicting the components of the splitter/electrospray interface with the different flows marked. All component parts are from commercially available sources as discussed previously [11]. The LC column effluent ("LC flow rate") is split into two flows: one enters a fused silica tube which also serves as the ionization tip for the microelectrospray source (Flow A, or "MS flow rate"); and the other is directed around the entrance of the capillary and into the branched portion of the outer stainless steel tube (Flow B). In many experiments, Flow B serves as a waste flow, but it also can be directed to another detector or to a fraction collector. The rate of Flow A is greatly reduced from the LC flow rate, and is also significantly lower than that of Flow B (typically 2000-fold). The flow rate in Flow A is controlled by the dimensions of the fused silica tip as well as the back pressure generated by an adjustable needle valve on the outlet tubing of Flow B.

The nanosplitter used here is similar to the original design with only a few minor changes. First, it was mounted onto a lab jack so that it could be easily moved from instrument to instrument, instead of being confined to Finnigan instruments with similar front end source mountings. The sliding rail component was again used to provide fine adjustment to the positioning of the interface. The most significant design change was in the attachment of the high voltage line. The original design [11] made electrical contact through an alligator clip placed directly onto the stainless steel tube of the nanosplitter. In the present design, a Valco zero dead volume union was incorporated into the interface and the high voltage was applied by connecting the line to a stainless steel clip

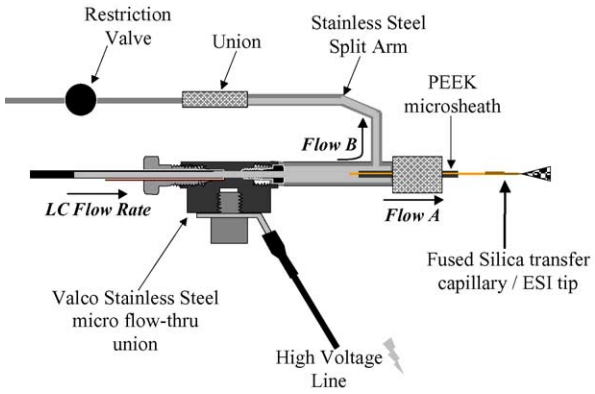

Fig. 1. Schematic of the post-column concentric splitting and microelectrospray elements of the nanosplitter with flow paths marked (positioning/mounting components not shown).

and screw mounted into the center of the union (i.e., a liquid junction connection). This design provides better electrical contact with the bulk liquid flow.

2.2. Indinavir/ritonavir competition

Two protease inhibitors, indinavir and ritonavir, were used to investigate the effects of varying the concentrations of mixture components on signal. One analyte was held at 1 μg/mL while the other was varied from 0.1 to 50 μg/mL. This produced two data sets from which to construct calibration curves, one that simulates indinavir as the internal standard (IS) and one that models ritonavir as the IS.

All experiments were conducted using a Hewlett-Packard 1090 liquid chromatograph (now Agilent Technologies, Wilmington, DE) coupled on-line to a Finnigan TSQ700 triple quadrupole mass spectrometer (now Thermo Electron Corporation, San Jose, CA). The MS was calibrated and tuned at 50 μL/min using a standard mixture of the peptide MRFA and the protein myoglobin. Each solution was run at 200 μL/min through a 2.1 mm × 30 mm HPLC column (Waters Symmetry C18, 3.5 μm, Milford, MA). Then, either the entire flow was introduced into the mass spectrometer or the flow into the mass spectrometer was decreased to 0.1 μL/min.

The LC analysis was conducted under isocratic conditions at 90% acetonitrile/10% 5 mM ammonium acetate (pH 4.4). These conditions were manipulated to ensure co-elution in order to investigate the signal properties of each analyte in the presence of the other. Each run consisted of three individual injections of 10 μL of the same sample. The mass spectrometric conditions were as follows: selected ion monitoring (SIM) in the positive mode using Q1 of *m/z* values 614.4 ($[M + H]^+$ of indinavir) and 721.3 ($[M + H]^+$ of ritonavir); total scan time of 1 s; electron multiplier set to 800 V. Some MS parameters were varied slightly to accommodate the different interfaces. The standard interface conditions were: capillary temperature: 200 °C; capillary voltage: 4.5 kV; sheath gas: nitrogen at 30 psi. The spray current for this interface was approximately 1.6 μA. The conditions of the nanosplitter were adjusted as follows: capillary temperature: 180 °C; capillary voltage: 1.8 kV; no sheath gas was necessary given the low flow. The spray current for the nanosplitter was approximately 0.4 μA.

2.3. Glyburide/GSK-A

A test compound, glyburide, and a proprietary GlaxoSmithKline compound (GSK-A) were used for a set of calibration samples with GSK-A as the internal standard. Analyte and internal standard were spiked into pooled human plasma, and the samples were precipitated with 75/25 acetonitrile/10 mM ammonium acetate. The glyburide levels for this curve were 0.01, 0.02, 0.05, 0.10, 0.50, 1.0, 2.0, and 5.0 μg/mL. Each sample contained GSK-A at a concentration of 1.0 μg/mL. The samples were centrifuged and the supernatants were collected. No further sample clean up was conducted.

Experiments were also conducted on a Finnigan TSQ700 triple quadrupole mass spectrometer (San Jose, CA), operating in SRM mode. Liquid chromatographic separations were carried out using an Agilent 1090 liquid chromatograph (Wilmington, DE) on a 2.1 mm × 50 mm C18 column (Waters Symmetry, 3.5 μm, Milford, MA). The flow through the LC column was maintained at 200 μL/min, however with the nanosplitter, flow was split 2000:1 before introduction into the mass spectrometer. The MS flow rate using the nanosplitter was approximately 0.1 μL/min, as determined by measurements made using a graduated microliter glass capillary and a stopwatch. The LC solvents used were 10 mM ammonium acetate and methanol. The LC pump was run in isocratic mode, with 70% methanol, 30% 10 mM ammonium acetate and the injection volume was 25 μL. The samples were analyzed using the same LC conditions and MS scanning parameters, with only the source parameters changed.

The mass spectrometer was operated in selected reaction monitoring mode to scrutinize two transitions, *m/z* 494.3 → 369.0 for glyburide, and *m/z* 429.2 → 228.2 for GSK-A. The isolation width for each transition was ± 0.2 Dalton, and the total scan time was set to 0.4 s. An ICL program was written in order to switch between the two transitions and allowed the collision energy to be set to different values for each analyte. The collision energy was set to 18 eV for the glyburide transition, and 30 eV for the GSK-A transition. The conversion dynode was set to −15 kV, the electron multiplier value to 1200 kV and the collision cell held at a pressure of 1.0 Torr.

For the conventional interface, the spray voltage was set to 4.5 kV, the sheath gas at 30 arbitrary units, the auxiliary gas at 10 arbitrary units and the capillary temperature at 225 °C. This temperature must be raised in order to assist in the desolvation of the large volume of liquid entering the mass spectrometer. For the nanosplitter, the sheath and auxiliary gases were turned off, the capillary voltage was decreased to 1.6 kV, and the capillary temperature was lowered to 180 °C.

2.4. GSK-B/GSK-B-d_5 LC–MS experiments using Sciex API 365 mass spectrometer

Two compounds, GSK-B and its deuterated (GSK-B-d_5) analogue were spiked into rat plasma; GSK-B at the following levels: 5, 10, 25, 50, 100, 250, 500, 1000, 2500, and 5000 ng/mL; and GSK-B-d_5 at 500 ng/mL into each sample. The analytes were extracted from the plasma using the following protocol: 500 μL of acetonitrile/ammonium formate (10 mM, pH 3) (75/25, v/v) was added to 100 μL of each plasma sample. The tubes were then capped and vortex mixed for approximately 1 min. They were centrifuged for 15 min at approximately 3220 × *g*. Fifty microliters of the supernatant was removed from the tubes after centrifugation and diluted to 500 μL.

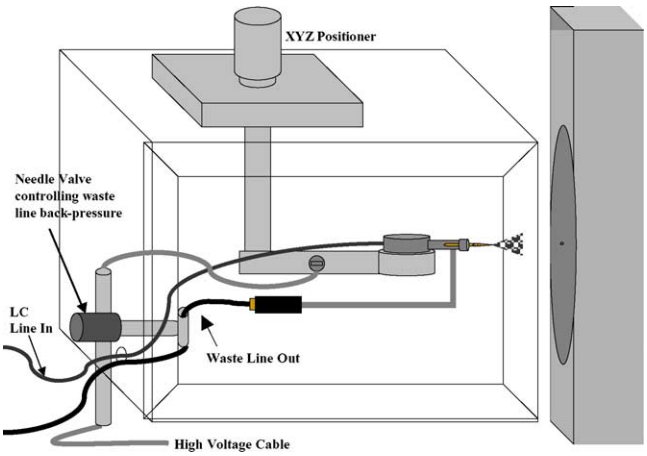

Fig. 2. Schematic of the nanosplitter interface fitted into the standard electrospray housing for a Sciex API 365 mass spectrometer.

Liquid chromatographic separations were carried out using a Flux Instrument AG Rheos 2000 pump (Basel, Switzerland). The LC column was an ACE 2.1 mm × 50 mm, 3 μm C18 column (Mac-Mod Analytical Inc., Chadds Ford, PA). The flow rate for these experiments was 500 μL/min through the LC column and the high MS flow (turbo ionspray), and 500 μL/min through the LC column and 0.2 μL/min into the mass spectrometer for the low MS flow (nanosplitter). The LC was run in isocratic mode, at 75% acetonitrile (solvent B), and 25% 10 mM ammonium formate (pH 3.0, solvent A). A 10 μL aliquot of the solution was injected via loop injection using a Leap Technologies CTC HTS PAL autosampler (Carrboro, NC).

The main components of the nanosplitter were fitted into a Sciex electrospray source housing, and the XYZ positioner and high voltage connections from the housing were used. For the nanosplitter, the ion spray voltage was set to 1500 V; the orifice voltage was set to 50 V and the CEM value was 2200 V. With the nanosplitter configuration (illustrated in the schematic Fig. 2), two switches needed to be triggered because the electrospray housing was pulled back to accommodate the nanosplitter and the curtain plate was removed for these analyses. For the turbo ionspray mode, the heater gas was set to 500 °C and the following voltages were used: ion spray voltage: 5000 V; orifice voltage: 60 V; and curtain plate voltage: 1050 V. With the turbo ionspray interface, the gases on the API-365 were set to the following values: nebulizer gas: 15 L/min; curtain gas: 10 L/min; turbo gas flow: 8.0 L/min). No gases were used with the nanosplitter. For both analyses, the mass spectrometer was run in positive polarity, SRM mode. The analyte transition monitored was from *m/z* 383.3 to *m/z* 248.0, and the d_5-internal standard was monitored from *m/z* 388.3 to *m/z* 248.0. Two "dummy" scans (from *m/z* 50 to 1000) were sandwiched between the analyte and internal standard transitions to minimize electronic cross talk in the mass spectrometer. The dwell times were 200 ms for the transitions and 50 ms for the dummy scans.

2.5. System optimization

In order to optimize the performance of the nanosplitter, it was necessary to adjust the inner diameter (i.d.) of the fused silica and width of the tip opening. Capillaries with i.d. of 75 μm demonstrated bubbling and spray instabilities, while those with an i.d. smaller than 20 μm plugged very easily. Plugging was also observed with wider bore capillaries that were pulled to very small tip widths. The optimal dimensions determined by systematic evaluation were 360 μm outer diameter, 20 μm inner diameter capillaries, pulled to a 10 μm tip. These tips produced very stable spray, reproducible split and no clogging under the experimental conditions employed here. If a significantly different split ratio should be desired, a tip with other dimensions may produce better results.

3. Results and discussion

3.1. Indinavir/ritonavir response and competition experiments

A comparison of the response curves for each analyte (indinavir or ritonavir) under two different experimental conditions was conducted to investigate analyte response across a range of concentrations. Each set of analyses produced two plots: (1) using the standard interface and introducing the entire flow (200 μL/min) from the LC column into the MS and (2) by replacing the standard interface with the nanosplitter and thereby, reducing the flow into the MS to 0.1 μL/min (the rest of the effluent split off to waste). For indinavir, the line equations were $y = 8 \times 10^6 x + 1 \times 10^8$ ($n = 3$, $R^2 = 0.9823$) and $y = 1 \times 10^8 x + 2 \times 10^9$ ($n = 3$, $R^2 = 0.9913$) using the standard interface and the nanosplitter, respectively. For ritonavir, the equation for the conventional interface was $y = 4 \times 10^7 x + 2 \times 10^9$ ($n = 3$, $R^2 = 0.9802$) and for the nanosplitter: $y = 7 \times 10^8 x + 2 \times 10^{10}$ ($n = 3$, $R^2 = 0.9649$). These line equations represent non-normalized experimental conditions, i.e., there was no internal standard used, thus the line equations

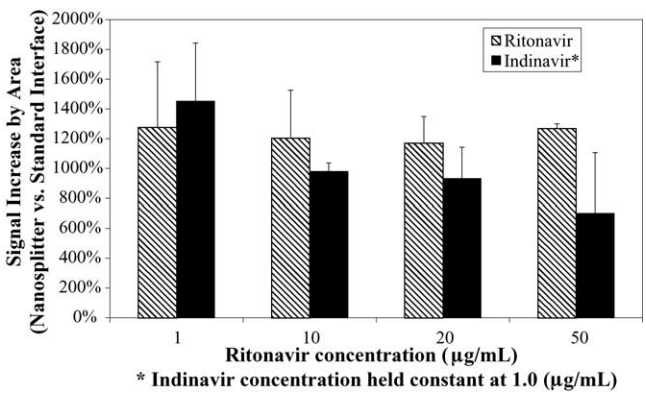

Fig. 3. Signal percent increases gained by each analyte for when the analyses of each sample by LC–MS with the standard interface and by LC–MS with the nanosplitter interface.

have exceptional intercept values. The changes in the slopes reflect the increase in the sensitivity when the flow was split 2000:1. These increases are quite dramatic, greater than an order of magnitude for each compound and represent overall signal increases of 12.5 times the peak area for indinavir and 17.5 times for ritonavir, despite the "removal" of 99.95% of the mass of the analyte (extrapolated from measurement of the flow split off by the nanosplitter).

In addition to the signal gain achieved when using the nanosplitter, the percent signal increase was also calculated for samples containing two analytes competing for ionization. In the experiment depicted in Fig. 3, the ritonavir concentration was varied from 1.0 to 50 μg/mL, while the concentration of indinavir was held constant at 1.0 μg/mL in each sample. As shown in the graph, the percent signal increase of ritonavir was of the same order of magnitude regardless of the concentration introduced. However, increasing the ritonavir concentration decreased the magnitude of the gain in the indinavir signal. The experiment was repeated with the concentration of indinavir held constant (at 1.0 μg/mL), while the ritonavir concentration was varied from 0.1 to 50 μg/mL. The same trend was observed, where the species of increasing concentration progressively reduced the magnitude of the signal gain of the species held at a lower, constant concentration (data not shown). In effect, these experiments demonstrate that even under microelectrospray conditions, analytes at high concentration may suppress the signal of low abundance mixture components. Even taking this into consideration, the incorporation of the nanosplitter resulted in significant improvements in overall signal gain.

3.2. Glyburide/GSK-A

Once the ability of the nanosplitter to produce significant signal increases with various concentrations was confirmed, it was important to evaluate its performance under condi-

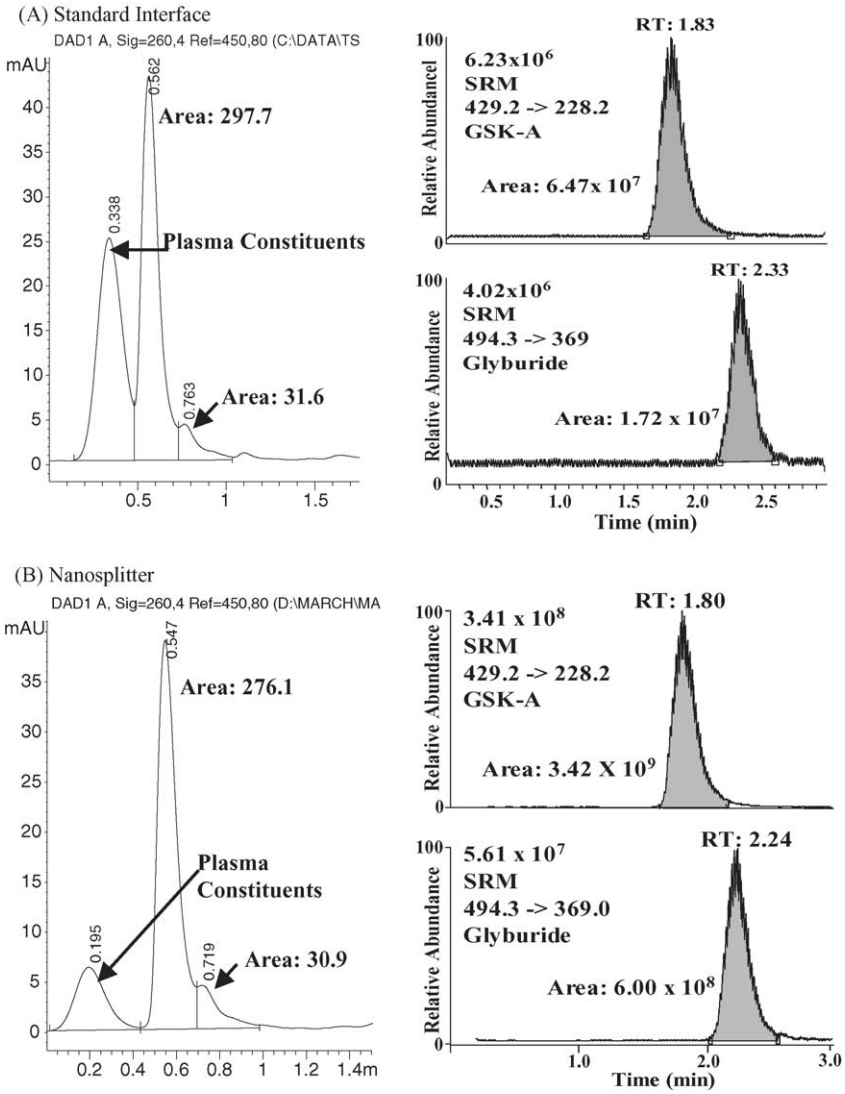

Fig. 4. Comparison of results from the photodiode array (*left panels*) and MS/MS (*right panels*) detections using the standard interface and nanosplitter for the mid-curve sample of glyburide and GSK-A.

tions typically encountered in the pharmaceutical industry, i.e., quantitative analysis from complex biological matrices. These experiments involved the construction of calibration curves through analysis of samples consisting of varied concentrations of an analyte in the presence of an internal standard.

The calibration plots for the analyses by the standard interface and nanosplitter were as follows: the standard interface curve equation: $y = 1.40 \times 10^{-3}x + 1.35 \times 10^{-2}$ ($n = 6$, $R^2 = 0.999$), the nanosplitter: $y = 1.9 \times 10^{-3}x + 4.18 \times 10^{-2}$ ($n = 9$, $R^2 = 0.999$). These results established the linearity of the nanosplitter over three orders of magnitude. The lower limit of quantification of the methodology was decreased from 0.05 to 0.01 μg/mL when using the nanosplitter, a five-fold improvement. Representative peaks for each analyte analyzed with both interfaces are shown in Fig. 4. The peak shape was maintained at the higher signal level with the nanosplitter, which may be a result of the positioning of the entrance of the tip in relation to the parabolic profile of the analyte plug in the HPLC eluent. The extremely small inner diameter of the tip entrance may provide a "pure stream sampling" by sampling only the center of the plug, minimizing drag effects from the walls of the tubing and outer tube of the nanosplitter.

Table 1 summarizes the statistical information from the comparison of the samples run by LC–MS/MS utilizing the two interfaces. The deviations in the retention times of both the analyte and internal standards are consistent. In an effort to investigate the improvements in signal produced by using the nanosplitter, the internal standard samples were subjected to further statistics. The mean area and signal-to-noise ratio of all the internal standard samples were determined and their standard deviations were examined. The sampling for these statistics consisted of single injections for each method of all 11 calibration points, which may introduce some additional variations that would not be seen with eleven repetitive injections of the same sample. Additional discrepancies can be added to the statistics due to pipeting and other sample preparation techniques. However, these additional factors can be offset, since the variations would exist in both methods.

The rationale that variations were common to both methods were confirmed when the %R.S.D. values of the area and S/N ratio of the internal standard were examined. The mean values for the peak areas are 6.80×10^7 (standard interface, %R.S.D. = 29.7) and 3.32×10^9 (nanosplitter, %R.S.D. = 40.0). The high %R.S.D. values can be attributed to the variations discussed above, as well as to poor reproducibility in the injection volumes with the autosampler of Hewlett-Packard 1090 liquid chromatograph. While these values seem high, the amount of variation that can be theoretically attributed to the change in interface (with all other parameters constant) is the difference between the two values, 10.3%. The signal-to-noise ratios were 130 (%R.S.D. = 23.5%) for the standard interface versus 371 (%R.S.D. = 32.6%) for the nanosplitter. The increase in the %R.S.D. for the S/N ratio was 9.10%. In addition to the factors considered above, these statistics were representative of injections made over a course of 3 days with multiple electrospray tips and multiple repositionings of the nanosplitter interface.

Table 1
Summary of the statistical data taken from the analyses of the glyburide and GSK-3 by the standard interface and the nanosplitter

	Standard interface	Nanosplitter
%R.S.D. analyte retention time	0.87	0.74
%R.S.D. internal standard retention time	0.91	1.07
Mean internal standard area	6.80E + 07	3.32E + 09
%R.S.D. internal standard area	29.69	39.98[a]
Mean internal standard S/N	130	371
%R.S.D. internal standard S/N	23.5	32.6[a]

[a] Changes in %R.S.D. for the internal standard area between the two interfaces is 10.29% and changes in %R.S.D. for the internal standard S/N between the two interfaces is 9.1%.

The design of the Agilent 1090 liquid chromatography allowed for simple integration of an additional photo diode array (PDA) detector before the mass spectrometer. The incorporation of the PDA allowed for scrutiny of the peak shape before entering the mass spectrometer and, as a consequence, direct comparison between the PDA detection and MS detection of the same sample by the two methodologies. The results demonstrated that the integrity of the chromatographic effluent is fully retained just prior to entering the ionization source regardless of the interface, as shown in Fig. 4.

In order to further examine, the observed increases in peak area, absolute signal plots of the non-normalized glyburide signal were compared for the Finnigan standard interface and the nanosplitter. The standard interface plot was $y = 6 \times 10^5 x - 4 \times 10^7$ ($n = 6$, $R^2 = 0.993$). The nanosplitter produced

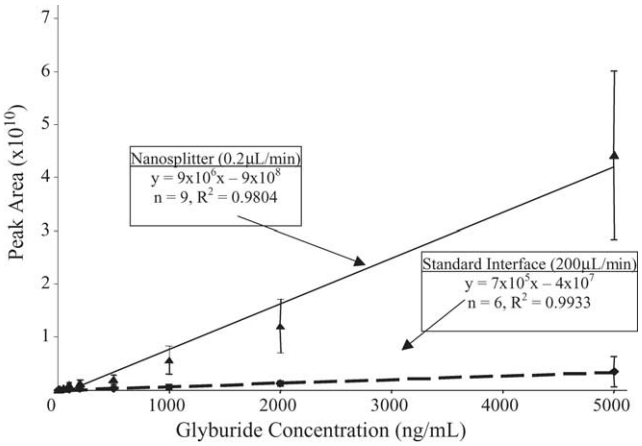

Fig. 5. Absolute signal response plots for glyburide analysis with each interface (no normalization to an internal standard). The steeper slope of the nanosplitter plot when compared to that of the standard interface line reflects the approximate 15-fold increase in sensitivity.

a plot of $y = 9 \times 10^6 x - 9 \times 10^8$ ($n = 9$, $R^2 = 0.980$), corresponding to a signal gain of 15, as shown in Fig. 5.

Another interesting observation made during these studies was the performance of the nanospray tip in the nanosplitter interface. Since there was minimal sample clean up, it may be expected that the "dirtiness" of the plasma samples would cause problems with the tips, such as clogging, and the spray would become unstable during the experiment. To the contrary, a single tip was used for 3 days (over 600 sample injections) with no signal degradation. This impressive performance may be explained by the use of the normal-bore column in the analysis, which may filter the samples. The high flow rate around the concentric split may have also served as a self-wash for the entrance of the spray tip, thus limiting clogging. Another possible contributing factor may be the dramatic decrease in mass loading, as the sample was split 2000:1 at the tip entrance.

3.3. GSK-B/GSK-B-d_5 LC–MS experiments using Sciex API 365 mass spectrometer

In order to assess the general utility of the nanosplitter, the interface was next coupled to a Sciex API 365 mass spectrometer, whose source design (turbo ionspray) differs significantly from that of the Finnigan TSQ 700 series. This comparison was of interest as it has been previously demonstrated that the ionization sources of different manufacturers' instruments showed variable susceptibility to ion suppression [21].

Due to the differences in source design, a number of features were altered or even removed to accommodate the interface on the Sciex API 365 mass spectrometer. First, a sensor was tripped because the nanosplitter did not allow for the electrospray housing to sit on the instrument as it normally would. Second, even when the electrospray interface is used on a Sciex API 365 MS, it is typically run at a few μL/min as its lowest flow as opposed to the nL/min used in microelectrospray. This is because lower spray becomes unstable with the turbo ionspray normal configuration. This instability has also been observed when using a nanosource on the Sciex API III + MS in our laboratory (data not shown). The instability of the submicroliter flow may be caused by the voltage applied to the curtain plate and the curtain gas itself. While high flow allows the spray to penetrate the field created by the voltage and the buffer zone of the gas, droplets from the lower flow may already be too small to "punch" through these regions. In order to counter that, the curtain plate was removed, and the curtain voltage and curtain gas were shut off when utilizing the nanosplitter.

A pair of compounds GSK-B/GSK-B-d_5 was analyzed by LC–MS to compare the performances of turbo ionspray operated with an MS flow rate of 500 μL/min and of the modified Sciex source incorporating the nanosplitter (MS flow of 0.2 μL/min). As with the TSQ 700 experiments, two quantitative comparisons were made. First a standard curve was constructed for GSK-B using GSK-B-d_5 as internal standard and, then the absolute response curve for GSK-B was determined. The equations of the respective standard calibration

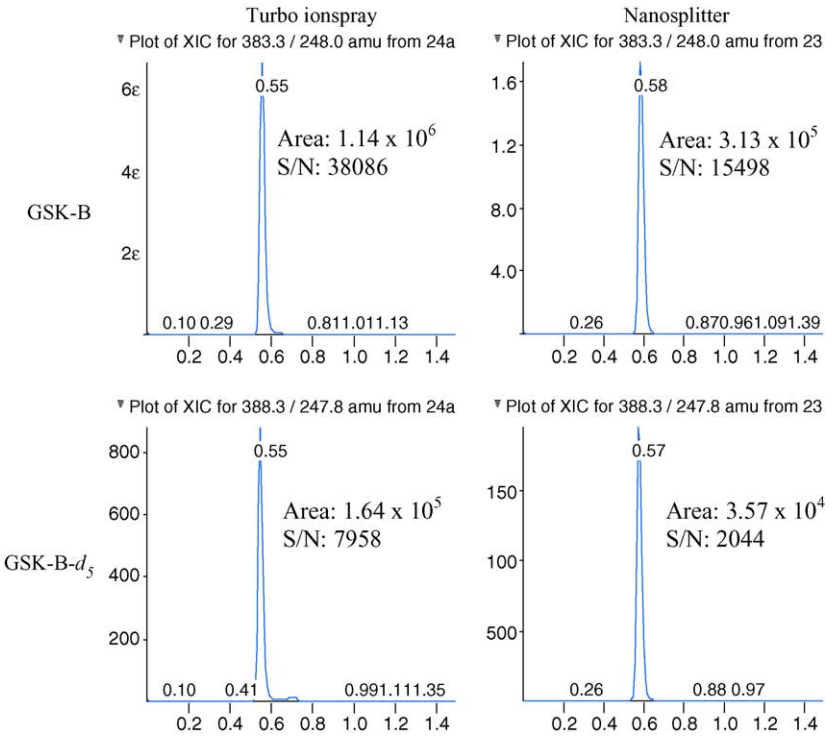

Fig. 6. Comparison of LC–MS/MS analyses of the 5000 ng/mL calibration sample by LC–MS utilizing the turbo ionspray and nanosplitter interfaces on the Sciex API 365 MS.

curves for the turbo ionspray and the nanosplitter were essentially identical: $y = 1.5 \times 10^{-3}x - 3.9 \times 10^{-3}$ ($n = 2$, $R^2 = 0.999$) for turbo ionspray and $y = 1.8 \times 10^{-3}x - 7.4 \times 10^{-3}$ ($n = 2$, $R^2 = 0.999$) for the nanosplitter. At the lowest GSK-B concentration used in the analyses (5 ng/mL), the S/N was 70 for the standard turbo ionspray interface and 45 for the nanosplitter. Chromatographic profiles for the analysis of the 5000 ng/mL sample (highest amount injected in each analysis) are shown in Fig. 6.

While the calibration curve equations using either interface were identical, distinct differences in absolute signal intensity were observed. Specifically, the response curves for GSK-B were $y = 230x + 4.39 \times 10^3$ ($n = 2$, $R^2 = 0.999$) and $y = 62.3x - 1.02 \times 10^3$ ($n = 2$, $R^2 = 0.999$) when using the turbo ionspray and the nanosplitter, respectively. Thus, contrary to the Finnigan instrument, the Sciex mass spectrometer fitted with the nanosplitter displayed a nearly four-fold signal loss when compared to turbo ionspray (slope ratio of 230:63 and S/N of 70:45 turbo ionspray:nanosplitter). Nevertheless, the numbers presented here reflect only a slight drop in signal with the nanosplitter, and the actual mass introduced into the MS is 2500 times less (as extrapolated from the flow rates). In fact, when the absolute signal curve was normalized to the mass introduced into the mass spectrometer, the slope of the nanosplitter curve was 6.23×10^3, compared to 24.0 for turbo ionspray, reflecting a net 270-fold gain in mass sensitivity. It is likely that any signal decrease upon incorporation of the nanosplitter is due, at least in part to the source design of the Sciex API 365 MS, which may not be well-suited for low flow sample introduction.

4. Conclusions

LC–MS/MS analyses using capillary LC columns are desirable to capitalize on the increased sensitivity of microelectrospray MS. Unfortunately, overloading of matrix constituents may rapidly deteriorate capillary columns and long run times have led analysts to pursue other methodologies. By utilizing a novel splitter/interface, we have shown that it is possible to combine normal-bore LC columns and microelectrospray mass spectrometry to form an integrated LC–MS system with improved performance on both sides of the "hyphen". Parameters investigated included the linearity, the dynamic range, and the sensitivity of the nanosplitter as compared to the standard interface. The nanosplitter produced calibration plots comparable to the standard interface, and demonstrated improvement of chromatographic performance. All plasma samples were prepared by simple protein precipitation with no rigorous sample clean up.

With a TSQ 700 series instrument, the increase in the absolute signal of test analytes was significant, with a signal gain of 15 times the peak area obtained using the standard interface. On a Sciex API 365 instrument, the nanosplitter virtually maintained the signal of the conventional turbo ionspray but did not exhibit significant improvement. Finnigan mass spectrometers incorporate a heated capillary design that seems to be beneficial in low flow analyses, while earlier MDS Sciex instruments, such as the API 365, do not. Researchers at MDS Sciex recently modified an API 3000 mass spectrometer to improve its performance at lower flow rates [39]. These modifications included modification of the geometry of the curtain plate, changing the application of the curtain plate potential and, perhaps more importantly, incorporating a heated laminar flow chamber. These changes led to significant improvement in analyte signal and ion counts, especially in the 100–1000 nL/min flow rate. Even without low flow optimization, the signal generated by the nanosplitter on the Sciex 365 instrument was 270× that of the turbo ionspray when the mass actually analyzed by the MS was accounted for. In addition, regardless of instrument, when using the nanosplitter, it was possible to recover 99.99% of the sample for further analysis, since only 0.01% of the sample was introduced into the mass spectrometer.

The robust design of the nanosplitter allows easy incorporation into the LC–MS laboratory. Since the split is concentric, and is incorporated into the electrospray ionization interface, undesired chromatographic effects are avoided. The ability to conduct fast, high flow LC separation while still increasing the sensitivity of the detection and recovering almost the entire sample offers unique opportunities for LC–MS analyses integrating the nanosplitter interface.

Acknowledgements

The authors appreciate the extensive contributions of Dr. Eric Gangl in the preparation of this manuscript, as well as those of Jimmy Flarakos. The authors would also like to thank the following individuals at GlaxoSmithKline Pharmaceuticals in King of Prussia, PA: Sherry Wang, David Lundberg, and Bob Miller. This work was supported in part by the National Institutes of Health, grant #1RO1CA69390. This is contribution No. 843 from the Barnett Institute.

References

[1] J. Abian, A.J. Oosterkamp, E. Gelpi, J. Mass Spectrom. 34 (1999) 244.
[2] B.L. Ackermann, M.J. Berna, A.T. Murphy, Curr. Top. Med. Chem. 2 (2002) 53.
[3] H. Cai, J.P. Kiplinger, W.K. Goetzinger, R.O. Cole, K.A. Laws, M. Foster, A. Schrock, Rapid Commun. Mass Spectrom. 16 (2002) 544.
[4] H. Iwabuchi, N. Kitazawa, H. Watanabe, M. Kanai, K. Nakamura, Biol. Mass Spectrom. 23 (1994) 540.
[5] N. Tyrefors, B. Hyllbrant, L. Ekman, M. Johansson, B. Langstrom, J. Chromatogr. A 729 (1996) 279.
[6] A. Tracqui, P. Kintz, B. Ludes, P. Mangin, J. Chromatogr. B: Biomed. Sci. Appl. 692 (1997) 101.
[7] P.J. Taylor, C.E. Jones, H.M. Dodds, N.S. Hogan, A.G. Johnson, Ther. Drug Monit. 20 (1998) 691.
[8] M.R. Fuh, C.J. Hsieh, J. Chromatogr. B: Biomed. Sci. Appl. 736 (1999) 167.

[9] S.W. Myung, H.K. Min, C. Jin, M. Kim, S.M. Lee, G.J. Chung, S.J. Park, D.Y. Kim, H.W. Cho, Arch. Pharm. Res. 22 (1999) 189.
[10] M. Rajanikanth, K.P. Madhusudanan, R.C. Gupta, Biomed. Chromatogr. 17 (2003) 440.
[11] E.T. Gangl, M.M. Annan, N. Spooner, P. Vouros, Anal. Chem. 73 (2001) 5635.
[12] M.R. Emmett, R.M. Caprioli, J. Am. Soc. Mass Spectrom. 5 (1994) 605.
[13] M. Wilm, M. Mann, Anal. Chem. 68 (1996) 1.
[14] R. Bonfiglio, R.C. King, T.V. Olah, K. Merkle, Rapid Commun. Mass Spectrom. 13 (1999) 1175.
[15] C.G. Enke, Anal. Chem. 69 (1997) 4885.
[16] B.K. Matuszewski, M.L. Constanzer, C.M. Chavez-Eng, Anal. Chem. 70 (1998) 882.
[17] R. King, R. Bonfiglio, C. Fernandez-Metzler, C. Miller-Stein, T. Olah, J. Am. Soc. Mass Spectrom. 11 (2000) 942.
[18] J.L. Sterner, M.V. Johnston, G.R. Nicol, D.P. Ridge, J. Mass Spectrom. 35 (2000) 385.
[19] S.A. Gustavsson, J. Samskog, K.E. Markides, B. Langstrom, J. Chromatogr. A 937 (2001) 41.
[20] T.M. Annesley, Clin. Chem. 49 (2003) 1041.
[21] H. Mei, Y. Hsieh, C. Nardo, X. Xu, S. Wang, K. Ng, W.A. Korfmacher, Rapid Commun. Mass Spectrom. 17 (2003) 97.
[22] Y. Hsieh, M. Chintala, H. Mei, J. Agans, J.M. Brisson, K. Ng, W.A. Korfmacher, Rapid Commun. Mass Spectrom. 15 (2001) 2481.
[23] A.T. Murphy, M.J. Berna, J.L. Holsapple, B.L. Ackermann, Rapid Commun. Mass Spectrom. 16 (2002) 537.
[24] X.S. Tong, J. Wang, S. Zheng, J.V. Pivnichny, P.R. Griffin, X. Shen, M. Donnelly, K. Vakerich, C. Nunes, J. Fenyk-Melody, Anal. Chem. 74 (2002) 6305.
[25] J. Schuhmacher, D. Zimmer, F. Tesche, V. Pickard, Rapid Commun. Mass Spectrom. 17 (2003) 1950.
[26] N.B. Cech, J.R. Krone, C.G. Enke, Anal. Chem. 73 (2001) 208.
[27] S. Zhou, K.D. Cook, J. Am. Soc. Mass Spectrom. 12 (2001) 206.
[28] T.R. Covey, E.D. Lee, J.D. Henion, Anal. Chem. 58 (1986) 2453.
[29] K. Heinig, F. Bucheli, J. Chromatogr. B: Anal. Technol. Biomed. Life Sci. 769 (2002) 9.
[30] J. Ayrton, R.A. Clare, G.J. Dear, D.N. Mallett, R.S. Plumb, Rapid Commun. Mass Spectrom. 13 (1999) 1657.
[31] A. Marchese, C. McHugh, J. Kehler, H. Bi, J. Mass Spectrom. 33 (1998) 1071.
[32] G. Shi, T.L. Lloyd, S.K. Sy, Q. Jiao, A. Wernicki, A. Mutlib, T.A. Emm, S.E. Unger, H.J. Pieniaszek Jr., J. Pharm. Biomed. Anal. 31 (2003) 937.
[33] C. Sottani, M. Bettinelli, M. Lorena Fiorentino, C. Minoia, Rapid Commun. Mass Spectrom. 17 (2003) 2253.
[34] T.K. Majumdar, R. Bakhtiar, D. Melamed, F.L. Tse, Rapid Commun. Mass Spectrom. 14 (2000) 476.
[35] T.K. Majumdar, S. Wu, F.L. Tse, J. Chromatogr. B: Biomed. Sci. Appl. 759 (2001) 99.
[36] A. Apffel, S. Fischer, G. Goldberg, P.C. Goodley, F.E. Kuhlmann, J. Chromatogr. A 712 (1995) 177.
[37] F.E. Kuhlmann, A. Apffel, S.M. Fischer, G.G. Goldberg, P.C. Goodley, J. Am. Soc. Mass Spectrom. 6 (1995) 1221.
[38] J. Yamaguchi, M. Ohmichi, S. Jingu, N. Ogawa, S. Higuchi, Anal. Chem. 71 (1999) 5386.
[39] B.B. Schneider, V.I. Baranov, H. Javaheri, T.R. Covey, J. Am. Soc. Mass Spectrom. 14 (2003) 1236.